

# On the nature of the $K_2^*(1430)$ , $K_3^*(1780)$ , $K_4^*(2045)$ , $K_5^*(2380)$ and $K_6^*$ as $K^*$ -multi- $\rho$ states

J. Yamagata-Sekihara<sup>1</sup> L. Roca<sup>2</sup> and E. Oset<sup>1</sup>

<sup>1</sup>*Departamento de Física Teórica and IFIC, Centro Mixto Universidad de Valencia-CSIC, Institutos de Investigación de Paterna, Aptdo. 22085, 46071 Valencia, Spain*

<sup>2</sup>*Departamento de Física. Universidad de Murcia. E-30071, Murcia. Spain*

February 23, 2024

## Abstract

We show that the  $K_2^*(1430)$ ,  $K_3^*(1780)$ ,  $K_4^*(2045)$ ,  $K_5^*(2380)$  and a not yet discovered  $K_6^*$  resonance are basically molecules made of an increasing number of  $\rho(770)$  and one  $K^*(892)$  mesons. The idea relies on the fact that the vector-vector interaction in s-wave with spins aligned is very strong both for  $\rho\rho$  and  $K^*\rho$ . We extend a recent work, where several resonances showed up as multi- $\rho(770)$  molecules, to the strange sector including the  $K^*(892)$  into the system. The resonant structures show up in the multi-body scattering amplitudes, which are evaluated in terms of the unitary two-body vector-vector scattering amplitudes by using the fixed center approximation to the Faddeev equations.

## 1 Introduction

The nature and structure of hadronic resonances is a prime issue in the understanding of the strong interaction. Besides the simplest quark-antiquark picture, other structures such as tetraquarks, glueballs or meson molecules may be dominant in the contribution to the wave function of some mesonic resonances. Regarding the meson molecule contribution, important milestones have been reached by the unitary extensions of chiral perturbation theory (UChPT), the chiral unitary approach. With the only input of lowest orders chiral Lagrangians and the implementation of unitarity in coupled channels, many resonances can be interpreted as meson-meson or meson-baryon molecules [1, 2, 3, 4, 5, 6, 7, 8, 9, 10], which are usually called dynamically generated resonances.

The use of vector mesons as building blocks within the chiral unitary approach has been recently considered both in the interaction of vector mesons with baryons [11, 12] and among themselves [13, 14, 15], starting from a lowest order hidden gauge symmetry Lagrangian [16, 17, 18, 19]. One of the main outputs of refs. [13, 14] was the very strong attraction of the s-wave vector-vector interaction with spin 2, to the point of generating dynamically the  $f_2(1270)$  and the  $K_2^*(1430)$  resonances, among others, as  $\rho\rho$  and  $K^*\rho$  molecules respectively with a very strong binding energy. Due to this strong attraction, in ref. [20] the issue of whether is it possible to obtain bound systems with increasing number of  $\rho$  mesons as building blocks was addressed. Indeed, it was found in ref. [20] that the resonances  $\rho_3(1690)$  ( $3^{--}$ ),  $f_4(2050)$  ( $4^{++}$ ),  $\rho_5(2350)$  ( $5^{--}$ ) and  $f_6(2510)$  ( $6^{++}$ ) are basically molecules of increasing number of  $\rho(770)$  particles. The multi-body interaction was written in terms of the two-body scattering amplitudes, using the fixed center approximation of the Faddeev equations (FCA) without the inclusion of any new free parameters.

The main aim of the present work is to extend the analysis of ref. [20] to the strange sector including the interaction of the  $K^*(892)$  resonance with several  $\rho(770)$  mesons since, as mention above, the  $\rho K^*$  interaction in s-wave and spin 2 is strongly attractive. Actually, it is strong enough to generate the  $K_2^*(1430)$  resonance as a  $K^*\rho$  quasibound state or molecule. Thus the main aim in the present work is, first, study the interaction of one  $K^*$  and two  $\rho$  mesons (the latter ones clustered in an  $f_2(1270)$ ) in order to see if some resonance structure shows up in the multi-body scattering amplitude. If this is the case, it could correspond to the  $K_3^*(1780)$  resonance. The procedure can be naturally extended including more  $\rho$  mesons into the system. Indeed, a  $\rho$  meson can be added to this generated  $K_3^*(1780)$  to try to see if in this four-body scattering amplitude there is evidence of a resonant structure that could be associated to the  $K_4^*(2045)$ , (it could also be found in  $f_2(1270)$ - $K_2^*(1430)$  interaction, which we will also study). Similarly, adding more  $\rho$  mesons we will study systems of one  $K^*$  and up to five  $\rho$  mesons to see, in the end, if the  $K_2^*(1430)$  ( $2^+$ ),  $K_3^*(1780)$  ( $3^-$ ),  $K_4^*(2045)$  ( $4^+$ ),  $K_5^*(2380)$  ( $5^-$ ) and a possible  $K_6^*$  ( $6^+$ ) resonances (the latter one not yet experimentally observed) are basically molecules made of an increasing number of  $\rho(770)$  and one  $K^*(892)$  mesons.

## 2 Two-body interaction: vector-vector unitarization

For the evaluation of the multi-body interactions that we are going to consider in the present work, one of the main ingredients is the two-body  $\rho\rho$  and  $K^*\rho$  unitarized scattering amplitudes. The unitarized  $\rho\rho$  amplitude is explained in detail in ref. [13] and summarized in ref. [20]. In the latter work the extension to evaluate the multi- $\rho$  scattering amplitudes was also explained. The main novelty of the present work with respect to ref. [20] is the inclusion of strangeness via the  $K^*$  resonance. For completeness, we briefly summarize here the model of [14] for the  $K^*\rho$  interaction. (We refer to [14] for further details.)

Following the ideas of the chiral unitary approach, the implementation of unitarity in the scattering amplitudes leads to the full two-body scattering amplitude for a given partial wave, which can be written by means of the Bethe-Salpeter equation in coupled channels:

$$t = V + VGt = (1 - VG)^{-1}V \quad (1)$$

where the kernel  $V$  is a matrix containing the tree-level vector-vector transition amplitudes (kernel of the Bethe-Salpeter equation) and  $G$  is a diagonal matrix which elements are the loop function for two vector mesons:

$$G = i \int \frac{d^4q}{(2\pi)^4} \frac{1}{q^2 - M_{V_1}^2} \frac{1}{q^2 - M_{V_2}^2}, \quad (2)$$

where  $M_{V_1}$  and  $M_{V_2}$  are the masses of the two vector-mesons of the corresponding channel. The widths of the vector mesons inside the loop  $G$  are taken into account by folding Eq. (2) with their spectral functions as explained in ref. [14]. The loop function in Eq. (2) can be regularized either with a three-momentum cutoff or with dimensional regularization. The equivalence of both methods for meson-meson scattering was shown in ref. [3]. In ref. [14] the regularization method was used with subtraction constants  $a_{\rho\rho} = -1.636$ , and  $a_{\rho K^*} = -1.85$ , chosen to get the right mass of the  $f_2(1270)$  and the  $K_2^*(1430)$  respectively. However, moderate changes in these parameters only produce small quantitative differences in the results [14]. The use of dimensional regularization with the subtraction constants given above, is equivalent to considering the cutoff method with a three-momentum cutoff of 875 MeV for  $\rho\rho$  and 1123 MeV for  $\rho K^*$ .

The contributions to the vector-vector potential  $V$  needed in Eq. (1), represented by a thick dot in Fig. 1, are depicted by the diagrams at the left

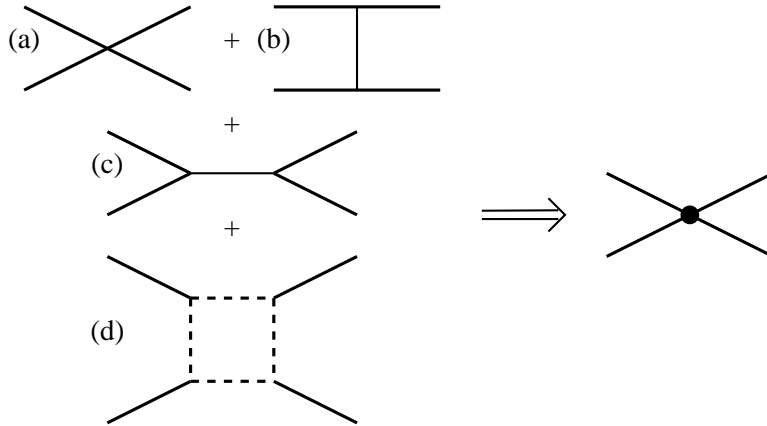


Figure 1: Mechanisms contributing to the kernel  $V$  (thick dot) of the Bethe-Salpeter equation, Eq. (1), for vector-vector scattering. Solid lines represent vector mesons and dashed lines pseudoscalar ones.

of Fig. 1. In this figure the solid lines represent vector mesons and the dashed lines pseudoscalar ones. The vertices needed to evaluate these diagrams are obtained from the hidden gauge symmetry Lagrangian [16, 17, 18, 19] for vector mesons. Actually we need the 4-vectors, 3-vectors and one vector–2-pseudoscalars contact terms. Explicit expressions for the Lagrangians and the  $V$ -matrix elements can be found in refs. [13, 14, 20]. The most relevant mechanisms are the contact term, Fig. 1a, and the  $t, u$  channel exchange, Fig. 1b. The  $s$ -channel, Fig. 1c, is very small since it is basically  $p$ -wave, and the box diagram, Fig. 1d, is relevant only for the width of the generated resonance [13, 14].

In the present work only the  $\rho\rho$  and  $K^*\rho$  interactions are needed. For the  $\rho\rho$  interaction with spin 2, the isospin 0 and 2 are possible. To the isospin 2 only the  $\rho\rho$  channel contributes, and to isospin 0 also  $K^*\bar{K}^*$ ,  $\phi\phi$ ,  $\omega\omega$  and  $\omega\phi$  contribute, but the dominant coupling of the generated  $f_2(1270)$  resonance is by far the  $\rho\rho$  [14]. This is one of the reasons why the  $f_2^*(1270)$  resonance is called a  $\rho\rho$  molecule or dynamically generated state from  $\rho\rho$  interaction. For  $K^*\rho$  interactions with spin 2 we have isospin 1/2 and 3/2. For isospin 1/2 the coupled channels needed are  $K^*\rho$ ,  $K^*\omega$  and  $K^*\phi$ , and for isospin 3/2 only  $\rho K^*$  is present. However, in isospin 1/2, the coupling of the generated resonance  $K_2^*(1430)$  to  $K^*\rho$  is about five times larger than to the other channels.

The  $\rho\rho$  and  $K^*\rho$  amplitudes needed in the present work are shown in

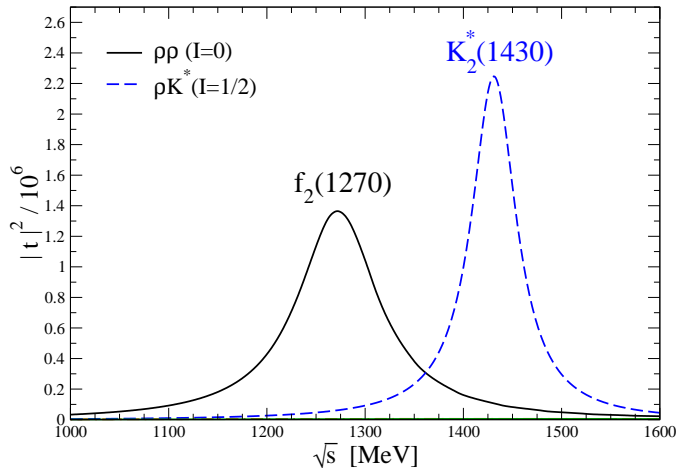


Figure 2: Modulus squared of the  $\rho\rho$  and  $\rho K^*$  scattering amplitudes

Fig. 2. The resonant structure for the  $f_2(1270)$  and  $K_2^*(1430)$  resonances are clearly visible in  $t_{\rho\rho}^{(I=0)}$  and  $t_{\rho K^*}^{(I=1/2)}$  respectively. The non-resonant amplitudes  $t_{\rho\rho}^{(I=2)}$  and  $t_{\rho K^*}^{(I=3/2)}$  are two orders of magnitude smaller compared to the resonant ones and thus are not visible in the figure.

### 3 Multi-body interaction

The formalism to evaluate the interaction for more than two vector mesons is similar to the one used in ref. [20]. In ref. [20] only  $\rho$  mesons were involved. However, in the present work we have two different species of particles,  $\rho$  and  $K^*$  resonances, which complicates a little bit the formalism. Therefore, in this section we only show the novelties due to the fact of having two different species and we refer the reader to ref. [20] for the rest of the formalism and for details.

We will illustrate the general process for the interaction of a generic particle  $A$  interacting with a cluster  $B$  made of two particles,  $b_1$  and  $b_2$ . For instance, in order to generate the  $K_3^*(1780)$  this would correspond to  $A = K^*$ ,  $B = f_2(1270)$  and  $b_1 = b_2 = \rho$ .

The basic idea is to use the fixed center approximation of the Faddeev equations (FCA) [22, 23, 24, 25, 26], which are written in terms of two partition functions  $T_1$ ,  $T_2$ , which sum up to the total scattering matrix,  $T$ ,

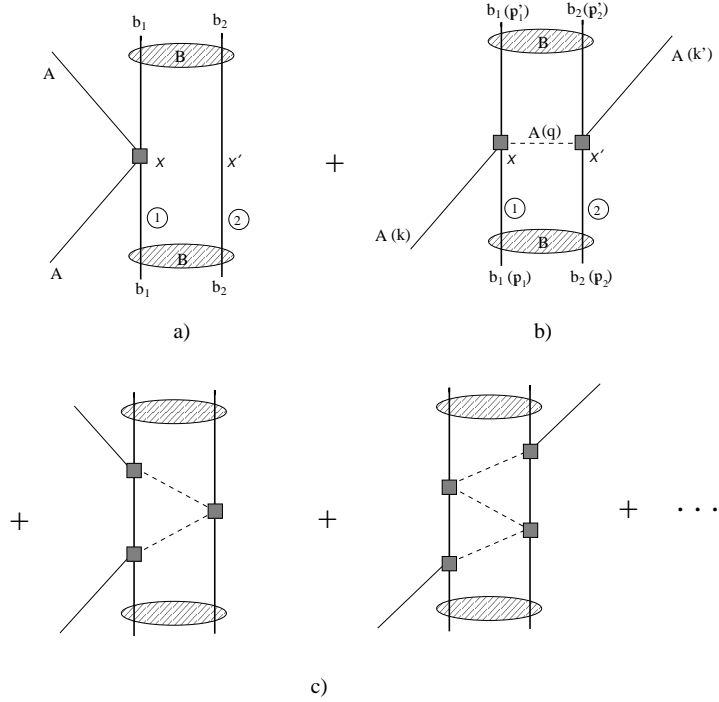


Figure 3: Diagrammatic representation of the fixed center approximation to the Faddeev equations for the interaction of a particle  $A$  with a particle  $B$  made of a cluster of two particles,  $b_1$  and  $b_2$ . Diagrams  $a)$  and  $b)$  represent the single and double scattering contributions respectively.

and read

$$\begin{aligned}
 T_1 &= t_1 + t_1 G_0 T_2 \\
 T_2 &= t_2 + t_2 G_0 T_1 \\
 T &= T_1 + T_2
 \end{aligned}
 \tag{3}$$

where  $T$  is the total scattering amplitude we are looking for,  $T_i$  accounts for all the diagrams starting with the interaction of the external particle  $A$  with particle  $b_i$  of the compound system  $B$  and  $G_0$  is the Green function for the exchange of a particle  $A$  between the  $b_1$  and  $b_2$  particles (dashed lines in Fig. 3). A schematic representation for the FCA of Eq. (3) is depicted in Fig. 3. The mechanism in Fig. 3a represents the single-scattering contribution ( $t_1$  in Eq. (3)) and Fig. 3b the double-scattering mechanism (the

next contribution,  $t1 = t1 + t1G_0t_2$ ). The addition of Fig. 3c represents the full resummation of mechanisms to get the full  $T_1$  partition function in the FCA. An analogous figure starting with the particle  $A$  interacting with  $b_2$  would account for the  $T_2$  amplitude.

For the evaluation of the two-body amplitudes,  $t_1$  and  $t_2$ , in terms of the unitarized vector-vector amplitudes in isospin basis of Eq. (1), one has to take into account that the particles involved are in given isospin states. We need first to consider the interaction of a  $K^*$  and a two- $\rho$  cluster. The two  $\rho$  mesons are in an isospin  $I = 0$  state,

$$|\rho\rho\rangle_{I=0} = -\frac{1}{\sqrt{3}}|\rho^+\rho^- + \rho^-\rho^+ + \rho^0\rho^0\rangle = \frac{1}{\sqrt{3}}\left(|(1, -1)\rangle + |(-1, 1)\rangle - |(0, 0)\rangle\right) \quad (4)$$

where the kets in the last member indicate the  $I_z$  components of the  $b_1$  and  $b_2$  particles,  $|(I_z^{(b_1)}, I_z^{(b_2)})\rangle$ . The external particle  $A$  is a  $K^*$  being in the state  $|(I_z^{(A)})\rangle$

$$|K^*\rangle = \left|\frac{1}{2}\right\rangle. \quad (5)$$

The interaction in terms of the two body potentials  $t_{Ab_1}$ ,  $t_{Ab_2}$  can be written as

$$\begin{aligned} T &= \left(\left\langle\frac{1}{2}\right|\otimes\frac{1}{\sqrt{3}}\langle(1, -1) + (-1, 1) - (0, 0)|\right)(t_{Ab_1} + t_{Ab_2}) \\ &\quad \left(\left|\frac{1}{2}\right\rangle\otimes\frac{1}{\sqrt{3}}|(1, -1) + (-1, 1) - (0, 0)\rangle\right) \\ &= \frac{1}{3}\left\langle\left(\left(\frac{3}{2}, \frac{3}{2}\right), -1\right) + \frac{1}{\sqrt{3}}\left(\left(\frac{3}{2}, -\frac{1}{2}\right), 1\right) + \sqrt{\frac{2}{3}}\left(\left(\frac{1}{2}, -\frac{1}{2}\right), 1\right) - \left(\left(\frac{1}{2}, \frac{1}{2}\right), 0\right)\right|t_{Ab_1} \right. \\ &\quad \left. \left|\left(\left(\frac{3}{2}, \frac{3}{2}\right), -1\right) + \frac{1}{\sqrt{3}}\left(\left(\frac{3}{2}, -\frac{1}{2}\right), 1\right) + \sqrt{\frac{2}{3}}\left(\left(\frac{1}{2}, -\frac{1}{2}\right), 1\right) - \left(\left(\frac{1}{2}, \frac{1}{2}\right), 0\right)\right\rangle\right. \\ &+ \frac{1}{3}\left\langle\frac{1}{\sqrt{3}}\left(\left(\frac{3}{2}, -\frac{1}{2}\right), 1\right) + \sqrt{\frac{2}{3}}\left(\left(\frac{1}{2}, -\frac{1}{2}\right), 1\right) + \left(\left(\frac{3}{2}, \frac{3}{2}\right), -1\right) - \left(\left(\frac{1}{2}, \frac{1}{2}\right), 0\right)\right|t_{Ab_2} \right. \\ &\quad \left. \left|\frac{1}{\sqrt{3}}\left(\left(\frac{3}{2}, -\frac{1}{2}\right), 1\right) + \sqrt{\frac{2}{3}}\left(\left(\frac{1}{2}, -\frac{1}{2}\right), 1\right) + \left(\left(\frac{3}{2}, \frac{3}{2}\right), -1\right) - \left(\left(\frac{1}{2}, \frac{1}{2}\right), 0\right)\right\rangle\right. \quad (6) \end{aligned}$$

where the notation followed in the last term for the states is  $\langle(I^{\text{total}}, I_z^{\text{total}}, I_z^k)|t_{ij}\rangle$ , where  $I^{\text{total}}$  means the total isospin of the  $ij$  system and  $k \neq i, j$  (the spectator particle).

This leads to the following amplitude for the single scattering contribution,

$$t_{\rho K^*} = \frac{1}{9}\left(4t_{\rho K^*}^{(I=\frac{3}{2})} + 5t_{\rho K^*}^{(I=\frac{1}{2})}\right). \quad (7)$$

In the evaluation of some of the amplitudes in the present work, we will also need to consider the interaction of a  $\rho$  meson and a  $K_2^*$  cluster. But in this case, the  $\rho K^*$  amplitude needed is different than Eq. (7) and the  $\rho\rho$  amplitude is different than in ref. [20] since now the cluster is a  $K^*\rho$  in isospin  $I = 1/2$ :

$$|\rho K_2^*\rangle_{I=\frac{1}{2}, I_z=\frac{1}{2}} = \sqrt{\frac{2}{3}} \left( |(1, -\frac{1}{2})\rangle - \frac{1}{\sqrt{3}} |(0, \frac{1}{2})\rangle \right) \quad (8)$$

where we have taken the  $I_z = 1/2$  for convenience and, in analogy to the nomenclature used in the equations above, the bracket represents  $(I_z^\rho, I_z^{K_2^*})$ . Therefore the  $\rho K$  inside the  $K_2^*$  can be in  $I_z = -1/2$  and  $I_z = +1/2$ , with the states given by

$$\begin{aligned} |\rho K^*\rangle_{I=\frac{1}{2}, I_z=-\frac{1}{2}} &= \frac{1}{\sqrt{3}} \left( |(0, -\frac{1}{2})\rangle - \sqrt{\frac{2}{3}} |(-1, \frac{1}{2})\rangle \right) \\ |\rho K^*\rangle_{I=\frac{1}{2}, I_z=+\frac{1}{2}} &= \sqrt{\frac{2}{3}} \left( |(1, -\frac{1}{2})\rangle - \frac{1}{\sqrt{3}} |(0, \frac{1}{2})\rangle \right) \end{aligned} \quad (9)$$

where now the bracket represents  $(I_z^\rho, I_z^{K^*})$ . Combining Eqs. (8) and (9) and proceeding analogously to Eq. (6) we get, after a bit of algebra, that the two-body amplitudes needed in the evaluation of the  $\rho K_2^*$  interaction are

$$\begin{aligned} t_{\rho\rho} &= \frac{2}{3} t_{\rho\rho}^{(I=0)} \\ t_{\rho K^*} &= \frac{1}{9} \left( 8 t_{\rho K^*}^{(I=\frac{3}{2})} + t_{\rho K^*}^{(I=\frac{1}{2})} \right). \end{aligned} \quad (10)$$

Note that, as mentioned above when explaining Fig. 2, the  $t_{\rho K^*}^{(I=\frac{3}{2})}$  term is negligible compare to  $t_{\rho K^*}^{(I=\frac{1}{2})}$  in spite of being multiplied by a factor 8 in the previous equation. The  $t_{\rho\rho}^{(I=0)}$  of Eq. (10) is evaluated with the unitary normalization for two identical  $\rho$  mesons (extra factor  $1/\sqrt{2}$ ) [13].

On the other hand, it is worth noting that the argument of the function  $T(s)$  in the FCA is the total invariant mass energy  $s$ , while the argument of  $t_1$  and  $t_2$  are  $s_1$  and  $s_2$ , where  $s_i (i = 1, 2)$  is the invariant mass of the interaction particle  $A$  and the particle  $b_i$  of the  $B$  molecule and is given by

$$s_i = m_A^2 + m_{b_i}^2 + \frac{1}{2m_B^2} (s - m_A^2 - m_B^2)(m_B^2 + m_{b_i}^2 - m_{b_{j \neq i}}^2), \quad (11)$$

where  $m_{A(B)}$  is the mass of the  $A(B)$  system and  $m_{b_i}$  is the mass of each building block of the  $B$  molecule.



In order to obtain the solution of the FCA, Eq. (3), in terms of the two-body amplitudes  $t_{Ab_i}$  and with the proper normalization, let us first consider the wavefunctions of the incident and outgoing  $A$  particle being plane waves normalized inside a box of volume  $\mathcal{V}$ . Then, following the same calculation as in ref. [20], the  $S$ -matrix for the single-scattering process of Fig. 3a is written as

$$S^{(1)} = -it_{Ab_1} \frac{1}{\mathcal{V}^2} \frac{1}{\sqrt{2\omega_{p_1}}} \frac{1}{\sqrt{2\omega_{p'_1}}} \frac{1}{\sqrt{2\omega_k}} \frac{1}{\sqrt{2\omega_{k'}}} \\ \times (2\pi)^4 \delta(k + k_B - k' - k'_B). \quad (12)$$

where the momenta are defined in Fig. 3b,  $\omega_p$  represents the on-shell energy of the corresponding particle with momentum  $p$  and  $k_B$  ( $k'_B$ ) represents the total momentum of the initial (final) cluster  $B$ .

The next contribution is the double scattering mechanism, which corresponds to Fig. 3b. Proceeding similarly to ref. [20] the  $S$ -matrix for this contribution takes the form

$$S^{(2)} = -i(2\pi)^4 \delta(k + K_B - k' - K'_B) \frac{1}{\mathcal{V}^2} \frac{1}{\sqrt{2\omega_k}} \frac{1}{\sqrt{2\omega_{k'}}} \frac{1}{\sqrt{2\omega_{p_1}}} \frac{1}{\sqrt{2\omega_{p'_1}}} \frac{1}{\sqrt{2\omega_{p_2}}} \frac{1}{\sqrt{2\omega_{p'_2}}} \\ \times \int \frac{d^3q}{(2\pi)^3} F(q, B) \frac{1}{q^0{}^2 - \vec{q}^2 - m_A^2 + i\epsilon} t_{Ab_1} t_{Ab_2}. \quad (13)$$

where  $F(q, B)$  is the form factor of the particle  $B$ , which represents essentially the Fourier transform of its wave function. Its derivation and further interpretation can be found in ref. [20] and its mathematical expression is given below, in Eq. (19).

On the other hand, the  $S$ -matrix of a general  $AB$  interaction can be written as

$$S = -it_{AB} (2\pi)^4 \delta(k + K_B - k' - K'_B) \frac{1}{\mathcal{V}^2} \\ \times \frac{1}{\sqrt{2\omega_k}} \frac{1}{\sqrt{2\omega_{k'}}} \frac{1}{\sqrt{2\omega_{k_B}}} \frac{1}{\sqrt{2\omega_{k'_B}}}. \quad (14)$$

Comparing Eq. (13) and (14), we can deduce the form that the FCA equations (3) take in our case

$$T_{Ab_1} = c_1 + c_1 \tilde{G}_0 T_{Ab_2} \\ T_{Ab_2} = c_2 + c_2 \tilde{G}_0 T_{Ab_1} \\ T = T_{Ab_1} + T_{Ab_2} \quad (15)$$

with

$$c_i = \frac{m_B}{m_{b_i}} t_{Ab_i}(s_i), \quad (16)$$

where we have taken  $\omega_{p_i} \simeq m_i$ , and <sup>1</sup>

$$\tilde{G}_0(s; A, B) = \frac{1}{2m_B} \int \frac{d^3q}{(2\pi)^3} F(q; B) \frac{1}{q^0(s; A, B)^2 - \vec{q}^2 - m_A^2 + i\epsilon}. \quad (17)$$

In Eq. (17),  $q^0$  is

$$q^0(s; A, B) = \frac{s - m_A^2 - m_B^2}{2m_B} \quad (18)$$

and the form factor takes de form

$$F(q, B) = \frac{1}{\mathcal{N}} \int_{\substack{p < \Lambda' \\ |\vec{p} - \vec{q}| < \Lambda'}} d^3p \frac{1}{m_B - \sqrt{\vec{p}^2 + m_{b_1}^2} - \sqrt{\vec{p}^2 + m_{b_2}^2}} \\ \times \frac{1}{m_B - \sqrt{|\vec{p} - \vec{q}|^2 + m_{b_1}^2} - \sqrt{|\vec{p} - \vec{q}|^2 + m_{b_2}^2}}, \quad (19)$$

$$\mathcal{N} = \int_{p < \Lambda'} d^3p \frac{1}{\left(m_B - \sqrt{\vec{p}^2 + m_{b_1}^2} - \sqrt{\vec{p}^2 + m_{b_2}^2}\right)^2}. \quad (20)$$

In Eq. (19),  $\Lambda'$  represents a cutoff which has a similar physical meaning [20] as the three-momentum cutoff of the loop function of Eq. (2). For that reason we take for  $B = f_2$  and  $B = K_2^*$  the same values for  $\Lambda'$  as for the cutoffs mentioned below Eq. (2). For  $B = f_4$  and  $B = K_4^*$ , which we also need in the present work, in principle the  $\Lambda'$  could be different since the typical maximum momentum could be different. We have checked that changing reasonably the value of  $\Lambda'$  for these cases as done in ref. [20] the qualitative conclusions do not change and the quantitative differences are small.

The system of equations (15) can be algebraically solved and it gives for the final multi-body scattering amplitude

$$T_{AB} = T_{Ab_1} + T_{Ab_2} = \frac{c_1 + c_2 + 2c_1c_2\tilde{G}_0}{1 - c_1c_2\tilde{G}_0^2}. \quad (21)$$

---

<sup>1</sup>Note the factor 1/2 different in Eq. (17) with respect to Eq. (41) of ref. [20] due to the new, more general, formulation.

## 4 Results

The interactions that we consider in the present work, summarized in table 1, are the following. For three particles:  $A = K^*$ ,  $B = f_2 = (b_1 = \rho, b_2 = \rho)$  and  $A = \rho$ ,  $B = K_2^*$ , ( $b_1 = \rho, b_2 = K^*$ ). For four particles:  $A = f_2$ ,  $B = K_2^* = (b_1 = \rho, b_2 = K^*)$ . For five particles:  $A = K^*$ ,  $B = f_4 = (b_1 = f_2, b_2 = f_2)$  and  $A = \rho$ ,  $B = K_4^* = (b_1 = f_2, b_2 = K_2^*)$ . For six particles:  $A = K_2^*$ ,  $B = f_4 = (b_1 = f_2, b_2 = f_2)$  and  $A = f_2$ ,  $B = K_4^* = (b_1 = f_2, b_2 = K_2^*)$ . (By the number of particles above we mean the number of elementary vector mesons if each cluster or molecule is broken down into its vector meson constituents).

	$A$	$B (b_1 b_2)$
two-body	$\rho$	$K^*$
three-body	$K^*$	$f_2 (\rho\rho)$
	$\rho$	$K_2^* (\rho K^*)$
four-body	$f_2$	$K_2^* (\rho K^*)$
five-body	$K^*$	$f_4 (f_2 f_2)$
	$\rho$	$K_4^* (f_2 K_2^*)$
six-body	$K_2^*$	$f_4 (f_2 f_2)$
	$f_2$	$K_4^* (f_2 K_2^*)$

Table 1: Clusters considered in the evaluation of the multi-body interactions. (See Fig. 3 for nomenclature).

In Fig. 4 we show the modulus squared of the different multi-body scattering amplitudes. The dotted and dashed-dotted lines represent the calculation considering only the single scattering mechanism and are normalized to the peak of the solid lines, which represent the full amplitudes, for the sake of comparison of the position of the maxima. The resonant structure of the amplitudes is clearly evident in the plot, which can be associated to the resonances labeled in the figures with masses given by the position of the maxima.

In table 2 the values of the masses of our generated systems are shown in comparison with the experimental values at the PDG [21]. Note that the  $K_6^*$  resonance is not quoted in the PDG, therefore our results on this resonance are genuine predictions of our model. Furthermore, it is also worth mentioning that there is only one single experiment [27] reporting on the existence of the  $K_5^*(2380)$  and thus in the PDG it is quoted as “needs confirmation”.

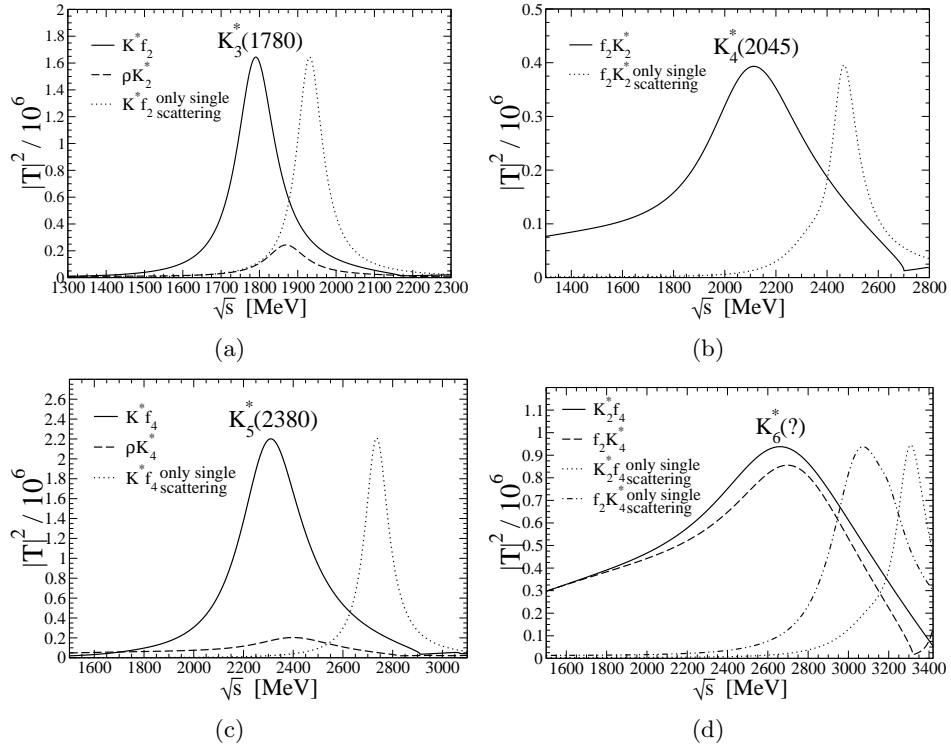


Figure 4: Modulus squared of the unitarized  $K^*$ -multi- $\rho$  amplitudes. The dotted and dashed-dotted lines have been normalized to the peak of the solid line for the sake of comparison of the position of the maxima

generated resonance	amplitude	mass, PDG [21]	mass only single scatt.	mass full model
$K_2^*(1430)$	$\rho K^*$	$1429 \pm 1.4$	–	1430
$K_3^*(1780)$	$K^* f_2$	$1776 \pm 7$	1930	1790
$K_4^*(2045)$	$f_2 K_2^*$	$2045 \pm 9$	2466	2114
$K_5^*(2380)$	$K^* f_4$	$2382 \pm 14 \pm 19$	2736	2310
$K_6^*$	$K_2^* f_4 - f_2 K_4^*$	–	3073-3310	2661-2698

Table 2: Results for the masses of the dynamically generated states. (All units are MeV)

The second column of table 2 indicates the dominant amplitude among those considered to get the resonance from which we take the position of the maximum. That amplitude is the one chosen to get the mass quoted in the table, from the position of the maximum. For instance, for the  $K_3^*$  we see in Fig. 4(a) that the  $K^* f_2$  squared amplitude is about seven times bigger than for  $\rho K_2^*$ . For the  $K_6^*$  both channels considered have almost equivalent strength, therefore both are considered in order to get the predicted mass of this resonance.

With only the single scattering mechanism, qualitative bumps for the resonances are produced but with masses that differ from the experimental values in about 200 – 400 MeV. The consideration of the multiple scattering processes in the FCA improves drastically the agreement with the experimental values of the masses. We have checked (not shown in Fig. 4) that only up to double scattering, Fig. 3a and b, the position of the masses do not improve significantly from considering only the single scattering. Therefore, the full resummation of Fig. 3c is crucial in order to get the full amplitude. This is a clear manifestation of the non-perturbative character of the Faddeev equations (3).

The agreement in the masses of our full model with the experimental values is remarkable, specially considering the large widths of these resonances. It is worth stressing the simplicity of our approach and the absence of parameters fitted in the model once the three-momentum cutoffs are chosen to get the right mass of the  $f_2(1270)$  and  $K_2^*(1430)$  resonances in the way explained below Eq. (2). Obtaining the widths of the generated resonances from the amplitudes is a more involved issue [20]. The widths of the bumps in the modulus squared of the amplitudes could in principle be associated to the resonance widths if they were Breit-Wigner like shapes, which is not

the case. It is worth stressing that our procedure produces the full amplitude, not only the resonant contribution. This means that the amplitudes contain also possible non-resonant or background contributions. The difference from Breit-Wigner shapes manifests the strong background produced by the non-linear dynamics of the non-perturbative calculation carried out in the present work. One has to consider that in a real experiment much of the strength of the amplitude would be associated to a background, which would reduce the width assigned to the resonance with respect the visual or apparent one. Taking this into account we can estimate semi-qualitatively the widths of the generated resonances as 120, 300, 300 and 600 MeV for  $K_3^*$ ,  $K_4^*$ ,  $K_5^*$  and  $K_6^*$  to be compared to the experimental values [21]  $159 \pm 21$ ,  $198 \pm 30$ ,  $178 \pm 37 \pm 32$  and *undetected* respectively. The width is also more sensitive to the value used in the cutoff of Eq. (19), (see the discussion below Eq. (20)). So the estimation of the widths must be considered only as qualitative. Regarding the  $K_6^*$ , it has not yet been discovered and thus we predict from our results a resonance  $I(J^P) = 1/2(6^+)$  with a mass about 2650 – 2750 MeV and width around several hundreds MeV. Certainly, this large width does not make its possible identification easy.

## 5 Conclusions

We show in the present work that the resonances  $K_2^*(1430)$ ,  $K_3^*(1780)$ ,  $K_4^*(2045)$ ,  $K_5^*(2380)$  and  $K_6^*$  are basically states made of one  $K^*(892)$  and an increasing number of  $\rho(770)$  resonances. The point is that the interaction between two vector mesons with spins aligned is very strong and, therefore, they tend to cluster. In particular, in refs. [13, 14] the  $\rho\rho$  and  $\rho K^*$  interaction was shown to be strong enough to bind the particles forming the  $f_2(1270)$  and the  $K_2^*(1430)$  resonances respectively. These vector-vector interactions were obtained by implementing the techniques of the chiral unitary approach with the only input of the lowest order vector-vector potential obtained from suitable hidden gauge symmetry lagrangians.

The multi-body amplitude in terms of the elementary vector-vector interactions is evaluated by solving the Faddeev equation in the fixed center approximation, which considers the interaction between three particles where two of them are clustered forming a resonance.

In the amplitudes obtained, there are significant bumps that can be associated to these specific resonances and we can obtain the mass from the position at the maxima. We get remarkable agreement in the mass of the resonances with the experimental values and give a prediction for the undis-

covered state  $K_6^*$ . It is also worth stressing the conceptual simplicity of the model and the non-inclusion of free parameters in the present work, once two regularization parameters are fixed in refs. [13, 14] to get the proper mass of the  $f_2$  and  $K_2^*$  resonances. It is clear that more states, like quark-antiquark, other meson-meson, several mesons, etc, can contribute to the wave functions of these resonances, but the fact that we get the resonances and in good agreement with experiment indicates that the many-vector-mesons components are dominant in the building up of the resonances studied in the present work.

Further experimental studies, specially about the not-yet discovered  $K_6^*$  and the poorly studied  $K_5^*(2380)$ , would be welcome to clarify the issue on the nature of these resonances. The success of the techniques used in the present work should also spur their future applications to other systems.

## Acknowledgments

We thank L. Geng and R. Molina for providing us the vector-vector amplitudes. This work is partly supported by DGICYT contracts FIS2006-03438, FPA2007-62777, the Fundación Séneca grant 11871/PI/09 and the EU Integrated Infrastructure Initiative Hadron Physics Project under Grant Agreement n.227431.

## References

- [1] N. Kaiser, P. B. Siegel and W. Weise, Phys. Lett. B **362**, 23 (1995).
- [2] J. A. Oller and E. Oset, Nucl. Phys. A **620** (1997) 438 [Erratum-ibid. A **652** (1999) 407].
- [3] J.A. Oller, E. Oset and J. R. Peláez, Phys. Rev. Lett. **80** (1998) 3452; ibid, Phys. Rev. D **59** (1999) 74001.
- [4] J. A. Oller and E. Oset, Phys. Rev. D **60** (1999) 074023.
- [5] N. Kaiser, Eur. Phys. J. A **3**, 307 (1998).
- [6] E. Oset and A. Ramos, Nucl. Phys. A **635** (1998) 99.
- [7] J. Nieves and E. Ruiz Arriola, Nucl. Phys. A **679**, 57 (2000).
- [8] J. A. Oller and U. G. Meissner, Phys. Lett. B **500**, 263 (2001).

- [9] C. Garcia-Recio, J. Nieves, E. Ruiz Arriola and M. J. Vicente Vacas, Phys. Rev. D **67**, 076009 (2003).
- [10] T. Hyodo, S. I. Nam, D. Jido and A. Hosaka, Phys. Rev. C **68**, 018201 (2003).
- [11] S. Sarkar, B. X. Sun, E. Oset and M. J. V. Vacas, Eur. Phys. J. A **44** (2010) 431.
- [12] E. Oset and A. Ramos, Eur. Phys. J. A **44** (2010) 445.
- [13] R. Molina, D. Nicmorus and E. Oset, Phys. Rev. D **78** (2008) 114018.
- [14] L. S. Geng and E. Oset, Phys. Rev. D **79**, 074009 (2009).
- [15] R. Molina, H. Nagahiro, A. Hosaka and E. Oset, Phys. Rev. D **80**, 014025 (2009).
- [16] M. Bando, T. Kugo, S. Uehara, K. Yamawaki and T. Yanagida, Phys. Rev. Lett. **54** (1985) 1215.
- [17] M. Bando, T. Kugo and K. Yamawaki, Phys. Rept. **164** (1988) 217.
- [18] M. Harada and K. Yamawaki, Phys. Rept. **381**, 1 (2003).
- [19] U. G. Meissner, Phys. Rept. **161**, 213 (1988).
- [20] L. Roca and E. Oset, Phys. Rev. D **82**, 054013 (2010).
- [21] C. Amsler *et al.* [Particle Data Group], Phys. Lett. B **667** (2008) 1.
- [22] L. D. Faddeev, Sov. Phys. JETP **12** (1961) 1014 [Zh. Eksp. Teor. Fiz. **39** (1960) 1459].
- [23] R. Chand and R. H. Dalitz, Annals Phys. **20**, 1 (1962)
- [24] R. C. Barrett and A. Deloff, Phys. Rev. C **60**, 025201 (1999).
- [25] A. Deloff, Phys. Rev. C **61**, 024004 (2000).
- [26] S. S. Kamalov, E. Oset and A. Ramos, Nucl. Phys. A **690**, 494 (2001).
- [27] D. Aston *et al.*, Nucl. Phys. B **296** (1988) 493.